HEWLETT PACKARD

Geometric Nonlinear Theory Quasi-Phase-Matching

Greg G. Luther, M.S. Alber*, J.E. Marsden†, J.M. Robbins
Basic Research Institute in the Mathematical Sciences
HP Laboratories Bristol
HPL-BRIMS-97-14
August, 1997

Geometric analysis of wave interactions is introduced to analyse type I and II quasi-phase-matched second-harmonic generation. Optimum strategies for light conversion are obtained using this geometric point of view.

*Department of Mathematics, University of Notre Dame, Notre Dame, Indiana
†Control and Dynamical Systems 116-81, California Institute of Technology, Pasadena, California

GEOMETRIC NONLINEAR THEORY OF QUASI-PHASE-MATCHING

G. G. Luther,[a,b,c,*] M. S. Alber,[c] J. E. Marsden[b] and J. M. Robbins[a,d]

[a] The Basic Research Institute in the Mathematical Sciences (BRIMS),
Hewlett-Packard Laboratories,
Filton Road, Stoke Gifford, Bristol BS12 6QZ, UK
[b] Control and Dynamical Systems 116-81, Caltech, Pasadena, CA 91125
[c] Department of Mathematics, University of Notre Dame, Notre Dame, IN 46556
[d] School of Mathematics, University Walk, Bristol BS8 1TW UK

July 19, 1997

Abstract

Geometric analysis of wave interactions is introduced to analyze type I and II quasi-phase-matched second-harmonic generation. Optimum strategies for light conversion are obtained using this geometric point of view.

Armstrong, Bloembergen, Ducuing and Pershan[1] proposed that by modulating the sign of the susceptibility of a nonlinear material the phases of interacting light waves could be manipulated to control the flow of energy among interacting light waves. These ideas have been particularly successful for efficient conversion of light to the second-harmonic frequency.[2] In this letter we introduce a new way to understand the dynamics of resonantly coupled nonlinear waves that generalizes the construction of the Poincaré sphere. We use it to analyze quasi-phase-matched second-harmonic generation (SHG) and to obtain optimum conditions for energy transfer among interacting waves.

The geometric approach described here extends the theory of quasi-phase-matching.[1, 2, 3] In addition to generating explicit solutions, it provides a powerful geometric visualization of nonlinear-wave interaction dynamics. It enables a more complete understanding of techniques for controlling wave interactions and applies to a large class of resonant wave interactions. Though no approximations are needed beyond the development of the envelope equations themselves, asymptotic analysis is facilitated. The standard theory based on linear approximation[2] is reproduced and given a geometric interpretation.

Type II SHG among quadratically coupled, resonantly interacting light waves is modeled with the resonant three-wave equations given by[1]

$$\frac{dq_1}{dz} = i\Delta k q_1 + i\gamma_1 q_2 \bar{q}_3 \ , \tag{1}$$

$$\frac{dq_2}{dz} = i\Delta k q_2 + i\gamma_2 q_1 q_3 \ , \tag{2}$$

$$\frac{dq_3}{dz} = i\Delta k q_3 + i\gamma_3 \bar{q}_1 q_2 \ , \tag{3}$$

where each q_j is a complex wave amplitude, $\Delta k = k_2 - k_3 - k_1$ is the wave-vector mismatch, and each γ_j is proportional to the second-order susceptibility, $\chi^{(2)}$. These equations model type II SHG, where waves one and three at frequency ω propagate in different polarization states. As they interact they generate a third light wave at the second harmonic frequency, 2ω. The equations model type I or scalar SHG when all three waves are in the same polarization state. The equations simplify in this latter case since $q_1 = q_3$ and $\gamma_1 = \gamma_3$.

The three-wave equations have a scaled canonical Hamiltonian structure[4] with a cubic Hamiltonian, $H = -(\bar{q}_1 q_2 \bar{q}_3 + q_1 \bar{q}_2 q_3)/2 - (\Delta k/2) \sum_{j=1}^{3} |q_j|^2/\gamma_j$, and are written in the compact form $dq_j/dz = \{q_j, H\} = -2i\gamma_j \partial H/\partial \bar{q}_j$. The Hamiltonian and the Manley-Rowe relations, $K_1 = |q_1|^2/\gamma_1 + |q_2|^2/\gamma_2$, $K_2 = |q_2|^2/\gamma_2 + |q_3|^2/\gamma_3$, $K_3 = |q_1|^2/\gamma_1 + |q_3|^2/\gamma_3$, are constants of the motion. Any two of the K_j with H form a complete and independent set of conserved quantities in involution, so the system is Liouville-Arnold integrable.

Phase space representations are useful for understanding global properties of dynamical systems. The three-wave phase space has three complex, or equivalently six real dimensions, and is difficult to visualize. Below, symmetries of Eqs. (1)–(3) associated with the Manley-Rowe relations are used to reduce the phase space to surfaces in three real dimensions. This reduced representation of the dynamics is then used to visualize and analyze SHG and quasi-phase-matching.

The Manley-Rowe relations correspond to S^1 group actions or rotations in complex three-space, where each of the transformations, $(q_1, q_2, q_3) \rightarrow (q_1 \exp(i\theta), q_2 \exp(i\theta), q_3)$, $(q_1, q_2, q_3) \rightarrow (q_1, q_2 \exp(i\theta), q_3 \exp(i\theta))$, and $(q_1, q_2, q_3) \rightarrow (q_1 \exp(i\theta), q_2, q_3 \exp(-i\theta))$, leave Eqs. (1)–(3) invariant. The coordinates $X + iY = q_1 \bar{q}_2 q_3$, $Z_1 = |q_1|^2 - |q_2|^2$, and $Z_2 = |q_2|^2 - |q_3|^2$, are also invariants of these S^1 group actions. They generalize the Stokes parameters.[5] Letting $q_j = \rho_j \exp(i\theta_j)$, the coordinates X and Y may be regarded as the components of a vector of length $|2\rho_1\rho_2\rho_3|$ and polar angle $\Omega = (\theta_1 - \theta_2 + \theta_3)$, where Ω is the relative phase of the three waves. The coordinates Z_1 and Z_2 measure the intensity difference between the second-harmonic wave and each fundamental wave, so larger values of Z_2 and smaller values of Z_1 correspond to more light at the second harmonic. For type I SHG $Z_2 = -Z_1$. The dimension of the three-wave system is reduced from six to four by finding the equations of motion for the invariant coordinants (X, Y, Z_1, Z_2). The linear

relation between Z_1, Z_2, and the constants of motion K_1, K_2 are used to eliminate either Z_1 or Z_2, reducing the system to three dimensions. In what follows, the coordinates (X, Y, Z_2) are used (without loss of generality).

Following Kummer[6], the reduced equations are written as follows:

$$dW_j/dz = \nabla\phi \cdot (\nabla W_j \times \nabla H_r) \quad j = 1, 2, 3 \; . \tag{4}$$

Here the gradient ∇ is taken with respect to $\mathbf{W} = (X, Y, Z_2)$, and $\phi = (\gamma_2 + \gamma_3)(X^2 + Y^2) - \kappa(\delta - Z_2)(\gamma_3 K_2 + Z_2)(\gamma_2 K_2 - Z_2)$, where $\kappa = \gamma_1\gamma_2\gamma_3/(\gamma_2 + \gamma_3)^2$ and $\delta = \gamma_2 K_1 + \gamma_3(K_1 - K_2)$. The Hamiltonian expressed in terms of the invariant coordinates is the reduced Hamiltonian, $H_r = -X - (\Delta k/(\gamma_2 + \gamma_3))((\gamma_2 + \gamma_3)K_1 + \gamma_2 K_2 - Z_2)/2$. Expanding (4), the reduced three-wave equations are written explicitly as

$$\frac{dX}{dz} = -\Delta k Y \tag{5}$$

$$\frac{dY}{dz} = \Delta k X + \frac{\partial\phi}{\partial Z_2} \tag{6}$$

$$\frac{dZ_2}{dz} = -2(\gamma_2 + \gamma_3)Y \; . \tag{7}$$

They reduce to quadratures readily.

From the reduced equations (4), it is evident that ϕ is a constant of the motion. Indeed, if ϕ is expressed in terms of the wave amplitudes q_j, then $\phi = 0$ identically. Thus the reduced dynamics is confined to the *three-wave surfaces* defined by $\phi(X, Y, Z_2) = 0$. The family of three-wave surfaces is parameterized by the Manley-Rowe constants K_1 and K_2, the wave-vector mismatch Δk, and the nonlinear coupling coefficients γ_j. Each is a surface of rotation about Z_2. The reduced Hamiltonian H_r is also a constant of the motion. Thus the trajectories of the reduced equations are curves produced by intersecting the three-wave surfaces with level sets of H_r. Since H_r is linear, its level sets are the planes $Z_2 = mX + (\gamma_2 + \gamma_3)(K_1 + 2H_r/\Delta k) + \gamma_2 K_2$, where $m = 2(\gamma_2 + \gamma_3)/\Delta k$. They are parallel to the Y axis.

In Fig. 1 the reduced phase space for type II SHG is plotted. A typical trajectory is a closed loop in (X, Y, Z_2). Energy is converted from the fundamental to the second harmonic and back during one trip around the three-wave surface. Points at which the Hamiltonian planes are tangent to the three-wave surfaces are fixed points. For type I SHG, a similar surface is obtained, but singularities along $(X, Y) = (0, 0)$ are introduced as $K_2 \to K_1$ that correspond to homoclinic trajectories.

As the slope, m, of the Hamiltonian planes is varied, the qualitative nature of the dynamics changes. When m is small, the Hamiltonian planes and the orbits on the three-wave surfaces are nearly horizontal. The linear oscillation captured in Eqs. (5) and (6)

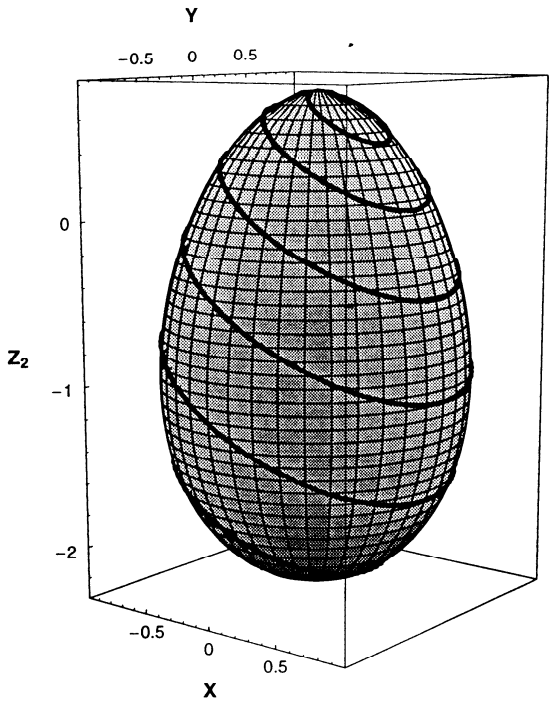

Figure 1: A reduced three-wave phase space for type II SHG on a three-wave surface. Here, $|m| = 3/5$, where $(\gamma_1, \gamma_2, \gamma_3) = (-1, -2, -1)$, $\Delta k = 10.0$ and $(q_1(0), q_2(0), q_3(0)) = (1.0, 0.05, 1.5)$.

dominates, and the dynamics is close to that of a driven harmonic oscillator with oscillation frequency Δk. This limit is achieved for instance when the system is far from phase matching. In the large-m limit, the orbits are nearly vertical. The nonlinear oscillation captured in Eqs. (6) and (7) dominates, and the dynamics is close to that of a cubic oscillator. When $\Delta k = 0$, the homoclinic orbit, where $H_r = 0$, produces maximum conversion. When $\Delta k \neq 0$, the orbit with the largest variation in Z_2 produces maximum conversion.[7] For intermediate values of m a trajectory has components of both the horizontal or linear oscillation and the vertical or nonlinear oscillation.

Quasi-phase-matching is achieved by alternating the signs of $\chi^{(2)}$ at every half period of the oscillation cycle, which for small m (the typical case) is half the linear oscillation period, *i.e.*, the coherence length $l_c = \pi/\Delta k$. Just as the second harmonic conversion saturates and begins to convert back to the fundamental, the direction of conversion is reversed by inverting the sign of $\chi^{(2)}$. The fundamental can then continue to convert into second harmonic. To understand quasi-phase-matching geometrically, construct the initial segment of a composite trajectory by intersecting the three-wave surface with the Hamiltonian plane corresponding to the initial data. Follow this trajectory for half of one period to a new position. Now let $\gamma_j \to -\gamma_j$ leaving everything else fixed. This transformation leaves the three-wave surface unchanged, but it reverses the sign of the slope of the Hamiltonian planes. To construct the next trajectory, intersect the three-wave surface with the Hamiltonian plane that passes through the new position after letting $\gamma_j \to -\gamma_j$. Follow this new trajectory half of one period. Continue this process constructing a composite trajectory for quasi-phase-matched SHG on the three-wave surface.

In Fig. 2 a type II quasi-phase-matched second-harmonic trajectory is plotted on a three-wave surface. It was generated by numerically solving Eqs. (1)–(3) and reversing the signs of the γ_j after integrating each distance l_c. The composite trajectory shown is the same as that obtained using the geometric construction described above. It spirals up the three-wave surface towards larger values of Z_2 as more light is converted to the second harmonic. The composite trajectory spirals because the direction of the nonlinear component of the rotation about the three-wave surface is reversed each time the signs of the γ_j are changed while the direction of the linear rotation remains unchanged. A similar picture is obtained in the case of type I second harmonic generation.

In order to produce maximum conversion from the fundamental to the second harmonic, choose the initial data at the point on the initial orbit that has the minimum value of Z_2. The maximum change in Z_2 for that orbit is then obtained after propagating half of one period. These initial points lie in the plane $Y = 0$ or $\Omega = n\pi$, where $n = 0, 2, 4, \ldots$ for $m > 0$ and $n = 1, 3, 5, \ldots$ for $m < 0$. Continue the construction of the composite quasi-phase-matched trajectory as before, changing the sign of the quadratic coefficients each time the plane $Y = 0$ is crossed. In a system where the second harmonic starts from noise, the growth of waves that are initially near the optimum relative phase is largest so this phase is picked automatically. In systems where the second harmonic is seeded, the

relative phase must be tuned to achieve optimum conversion.

The optimum conversion efficiency is closely approximated by choosing the initial data $Y = 0$, $X < 0$ for $(\gamma_1, \gamma_2, \gamma_3) = (-1, -2, -1)$ and $\Delta k > 0$ and taking steps of length l_c if m is small. As shown in Fig. 2, these conditions still produce excellent conversion efficiency after only 8 layers by choosing l_c even when $m = -0.3$. The nonlinear component of the oscillation contributes a small shift to the linear period, $2l_c$, as can be seen in Fig. 2. This shift leads to the eventual saturation of the quasi-phase-matched conversion. As m increases, the linear period is an increasingly poor approximation to the actual oscillation period and the quasi-phase-matched conversion saturates after only a few steps of length l_c. At these larger values of m, the signs of the quadratic coefficients must be alternated at half the *nonlinear* period to obtain the most efficient quasi-phase-matched conversion. Because this period varies as the harmonic grows, optimizing the conversion efficiency requires that the length of the polled sections be varied along the propagation path. If m is large enough, only a few layers are needed to produce complete conversion. The nonlinear periods are calculated using standard techniques (see also Ref. [7] for optimization of the linear mismatch of averaged wave systems). If the length of the polled sections can not be varied, corrections to both l_c and the initial relative phase give the constrained optimum conversion efficiency for the system.

The strategy for quasi-phase-matched SHG described above is only one of many possibilities for controlling energy flow in resonant wave interactions. For example, the second harmonic could be generated by moving through a small fraction of an orbit within each layer of material. In systems that have large m, or are nearly phase matched, this is accomplished by changing the sign of the phase mismatch parameter instead of the quadratic coefficients. This strategy is optimized by taking inital data that has relative phase nearly equal to $\Omega = n\pi/2$, $n = 1, 2 \ldots$, which is the opposite of the condition for conventional quasi-phase-matching. Geometrically, it corresponds to trajectories that move a fraction of a period at each step and zig-zag up the side of the three-wave surface along $X = 0$. Just as in conventional quasi-phase-matching a relatively small amount of conversion is obtained in each layer, while the net conversion can be quite large. In contrast to a single layer of nearly phase-matched material, this scheme introduces the possibility of manipulating higher-order terms to reduce unwanted effects.

For large m, linear approximations are typically only valid for fractions of an oscillation period. Only for orbits near fixed points at which a Hamiltonian plane is tangent to a three-wave surface do the reduced equations linearize, to yield a harmonic oscillator model that remains valid for times comparable to a period. As noted above, when m is small the orbits become nearly horizontal and the linear terms in Eqs. (5) and (6) dominate. The standard driven harmonic oscillator model described in Ref. [2] is obtained in this limit. It has a resonance at $\Delta k = 0$. By periodically polling the quadratic coefficient at half the linear oscillation period a kick is introduced, causing the harmonic to grow even though $\Delta k \neq 0$. This is analogous to pushing a pendulum at half its period. In this small-m limit the

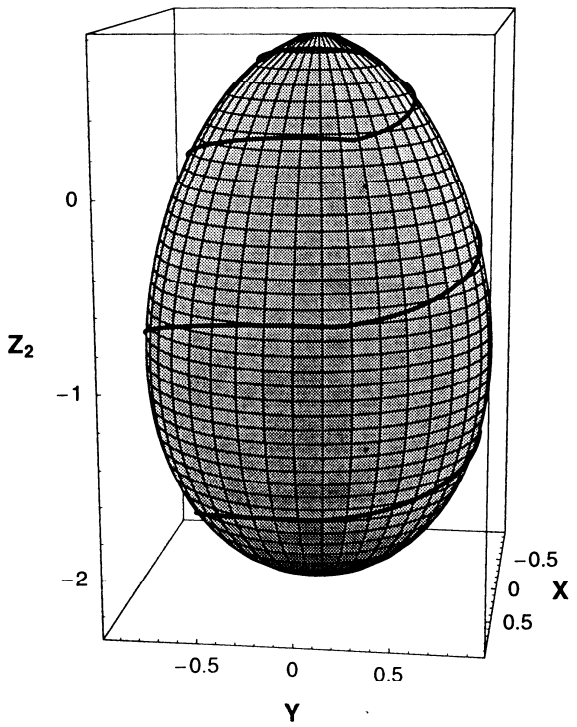

Figure 2: A composite trajectory with 8 sections of length $l_c = \pi/\Delta k$ for type II quasi-phase-matched SHG on a three-wave surface. Here, $|m| = 0.3$, where $(\gamma_1, \gamma_2, \gamma_3) = (-1, -2, -1)$, $\Delta k = 20.0$ and $(q_1(0), q_2(0), q_3(0)) = (1.0, 0.05, 1.5)$.

Hamiltonian planes generate orbits that are nearly horizontal over the entire three-wave surface. The driven oscillator model has a large region of validity, remaining valid even at large conversion efficiency. The oscillation period, therefore, is also well approximated by $2l_c$ over a large region of the three-wave surface.

A geometric theory of resonant three-wave interactions has been introduced and used to analyze quasi-phase-matched SHG. The theory extends to a broad class of resonant wave interactions and is a key element of a general understanding and analysis of nonlinear control strategies for them. This analysis underscores the idea that engineering the properties of dynamical systems can improve the net performance of optical materials.

GGL acknowledges helpful discussions with D. K. Serkland. MSA was partially supported by NSF grants DMS 9626672 and 9508711. GGL gratefully acknowledges support from BRIMS, Hewlett-Packard Labs and from NSF under grants DMS 9626672 and 9508711. JEM was partially supported by the Department of Energy under Contract DE-FG0395-ER25251.

* Present address: Engineering Sciences and Applied Mathematics Department, McCormick School of Engineering and Applied Science, Northwestern University, 2145 Sheridan Road, Evanston, Il 60208–3125.

References

[1] J. A. Armstrong, N. Bloembergen, J. Ducuing and P. S. Pershan, Phys. Rev. **127**, 1918 (1962).

[2] M. M. Fejer, G. A. Magel, D. H. Jundt and R. L. Byer, IEEE J. Quantum Electron. **QE-28**, 2631 (1992).

[3] K. C. Rustagi, S. C. Mehendale and S. Menakshi, IEEE J. Quantum Electron. **QE-18**, 1029 (1982).

[4] See for example: C. J. McKinstrie, and G. G. Luther, Phys. Lett. A **127**, 14 (1988).

[5] M. Born and E. Wolf, *Principles of Optics* (Pergamon, Oxford, 1980).

[6] M. Kummer, J. Math. Anal. and Apps. **52**, 64 (1975); *Stochastic behavior in classical and quantum Hamiltonian systems.* Springer Lect. Notes in Phys. **93**, (1979); J. Diff. Eqns. **83**, 220 (1990).

[7] C. J. McKinstrie, G. G. Luther and S. H. Batha, J. Opt. Soc. Am. B **7**, 340 (1990).